ELSEVIER

Journal of Organometallic Chemistry 545–546 (1997) 337–344

Journal of Organometallic Chemistry

Catalytic formation of carbamates and cyclic carbonates by copper complex of 2,5,19,22-tetraaza[6,6](1,1')ferrocenophane-1,5-diene X-ray crystal structure of [Cu(1)]PF_6

Hak-Soo Kim, Jeong-Won Kim, Soon-Chul Kwon, Sang-Chul Shim, Tae-Jeong Kim *

Department of Industrial Chemistry, Kyungpook National University, Taegu, 702-701, South Korea

Received 19 March 1997; received in revised form 3 June 1997

Abstract

The reaction of [Cu(MeCN)$_4$]PF_6 with a ferrocene-containing tetraazamacrocycle 2,5,19,22-tetraaza[6,6](1,1')ferrocenophane-1,5-diene (**1**) gives the copper(I) complex of the type [Cu(**1**)]PF_6 (**2**) which crystallizes in the orthorhombic system: $P2_12_12_1$ (#19); $a = 7.597(2)$ Å, $b = 14.805(5)$ Å, $c = 24.194(4)$ Å; $Z = 4$; $R = 0.080$; $R_w = 0.083$. The geometry around the central metal is a distorted tetrahedron with two pairs of differing Cu–N bond length. This complex has demonstrated the excellent catalytic activity toward the formation of cyclic carbonates and carbamates in the presence of CO_2, giving almost quantitative product yields in most reactions that have been employed. © 1997 Elsevier Science S.A.

Keywords: Ferrocene-containing macrocycle; Copper; Carbamates; Cyclic carbonates; CO_2 insertion

1. Introduction

The incorporation of carbon dioxide into organic substrates by transition metals in organic synthesis has attracted considerable attention due to its nontoxicity and low price as compared with carbon monoxide [1–3]. Of particular interest is the formation of carbamates and cyclic carbonates from the reaction of terminal alkynes as illustrated in Scheme 1, since these are useful chemicals for agriculture or starting products for organic synthesis. In addition, these were used as natural and synthetic polymers such as lignin, cellulose ester, nylon and polyvinyl chloride [4–8].

The formation of cyclic carbonates is now known to be catalyzed by various transition metal complexes such as CuCl, Cu(acetate)$_2$, $CuCl_2$ [9–12], $Ru_3(CO)_{12}$ [13], $Pd(PPh_3)_4$ [14], and $CoCp_2$ [15]. Even simple phosphines such as PR_3 (R = Bu, Ph, Me, etc.) are known to catalyze this transformation in high yields (50–98%) [4,5]. Carbamates are obtained from the reaction of terminal alkynes with secondary amines by ruthenium

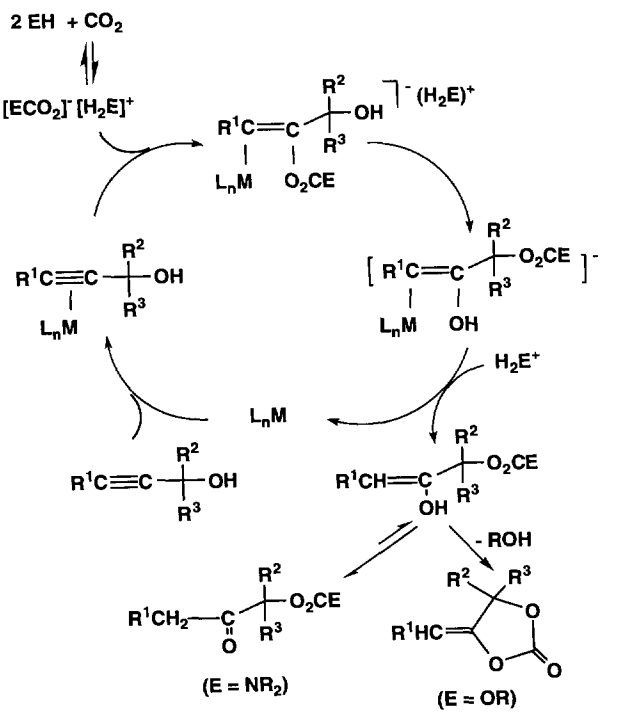

Scheme 1.

* Corresponding author.

PII S0022-328X(97)00366-5

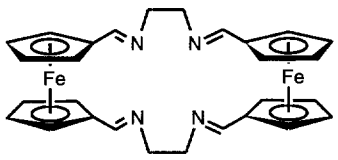

(1)

Scheme 2.

or iron catalysis as reported in Refs. [4,5,16–19]. In the case of iron catalysis, the ligand employed was 1,1′-bis(diphenylphosphino)ferrocene.

These findings and the fact that ferrocene-based phosphines and amines have found wide applications as ligand for complexes in a number of homogeneous catalytic reactions and asymmetric syntheses [20–25] have led us to design and synthesize a series of ferrocene-containing polyazamacrocycles, one of which is shown in Scheme 2 [26].

From a redox view point, ferrocene-containing macrocycles and cryptands have attracted considerable attention in recent years due to their potential applications in the fields of molecular ferromagnets [27,28], molecular sensors [29,30], nonlinear optics [31–35], and even as catalysts either in chemical processes or as mimics for metallo-enzymes [36–41]. In addition, one of the reasons for our interest in these systems lies in the fact that heteropolymetallic assemblies consisting of these macrocyclic ligands (redox-active centers) and metal ion (Lewis acid) are expected to afford intriguing prospects for small molecule activation [42–45]. They may serve as multielectron redox mediators in the redox–catalytic reactions.

This paper describes the synthesis and X-ray crystal structure of **2** and its catalytic application to the formation of cyclic carbonates and carbamates from terminal alkynes in the presence of CO_2.

2. Experiment

2.1. General technique

All manipulations were carried out under an argon atmosphere using a double manifold vacuum system and Schlenk techniques. All commercial reagents were used as received unless otherwise mentioned. Solvents were purified by standard methods and were freshly distilled prior to use. Microanalyses were performed by the Center for Instrumental Analysis, Kyungpook National University. $^1H\{^{31}P\}$ NMR spectra were recorded on a Varian Unity Plus 300 spectrometer operating at 300, 121.5 MHz, respectively. IR spectra were recorded on a Mattson FT-IR Galaxy 6030E spectrophotometer and Nicolet Magna-IR 550 spectrometer. UV–Visible spectra were measured on a HP 8452A diode-array spectrophotometer. The ligand 1,1′-bis(diphenylphosphino)ferrocene (dppf) [46], ferrocene-1,1′-dicarboxaldehyde [47], 2,5,19,22-tetraaza[6,6](1,1′)ferrocenophane-1,5-diene (**1**) [26,48], and $[Cu(CH_3CN)_4][PF_6]$ [49] were prepared according to the literature methods. Structure determinations of carbamates [50], cyclic carbonates [15], and polycarbonate [51,52] were performed by usual spectroscopic and microanalytical techniques as reported in the literature.

2.2. Preparation of 2

To a suspension of $[Cu(MeCN)_4][PF_6]$ (0.30 g, 0.80 mmol) in CH_2Cl_2 (10 ml) was added dropwise a solution of **1** (0.37 g, 0.80 mmol) in CH_2Cl_2 at ambient temperature through a pressure-equalizing dropping funnel. The mixture was stirred for 1 h during which time red precipitates were formed. These were filtered off, washed with CH_2Cl_2 (3 × 5 ml) and recrystallized from CH_3CN/diethylether to afford dark red crystals (4.0 g, 69%). Anal. calc. (found) for $C_{28}H_{28}N_4PF_6Fe_2Cu$: C, 45.40 (45.43); H, 3.81 (3.72); N, 7.56 (7.63). IR (KBr/Nujol, cm^{-1}): 1629 ($\nu_{C=N}$, vs), 854vs/520s (ν_{PF}). ^1H NMR ($CDCl_3$, δ): 3.90 (s, 8H, CH_2), 4.49s/4.63s (16H, AB, C_5H_4), 8.57 (s, 4H, N=CH).

2.3. Preparation of $[Cu(dppf)(MeCN)_2][PF_6] \cdot CH_2Cl_2$ (3)

A solution of dppf (0.47 g, 0.85 mmol) in 10 ml of CH_2Cl_2 was added dropwise, through a pressure-equalizing dropping funnel, to a suspension of $[Cu(MeCN)_4][PF_6]$ (0.32 g, 0.85 mmol) in 10 ml of CH_2Cl_2. The reaction mixture was stirred at room temperature for 1 h. The volume of solvent was reduced to half an amount followed by the addition of diethyl ether (10 ml) to afford yellowish brown crystals on cooling (0.54 g, 75%). Anal. calc. (found) for $C_{36}H_{34}N_2P_3F_6Fe_2Cu_1 \cdot CH_2Cl_2$: C, 50.37 (50.82); H, 3.91 (3.99); N, 3.01 (2.67). IR (KBr/Nujol, cm^{-1}): 2306w/2271w (ν_{MeCN}), 840vs/557s (ν_{PF}). ^1H NMR ($CDCl_3$, δ): 7.43–7.47 (m, 20H, Ph), 5.30 (s, 2H, CH_2Cl_2), 4.15s/4.36s (8H, AB, C_5H_4), 2.12 (s, 6H, MeCN). ^{31}P NMR ($CDCl_3$, δ): −11.87s.

2.4. Catalysis

Under a stream of nitrogen, acetylenic alcohol substrate (5 mmol), base (0.5 mmol), and catalyst precursor (0.05 mmol) were placed in an autoclave (50 ml). After purging with CO_2 a few times, the reactor was pressurized to the desired pressure ($P(CO_2)$ 38 atm). The

system was heated at 100°C for 24 h after which the reaction was terminated by rapid cooling, and then the reactor was discharged. After passing the reaction mixture through a short silicagel column to remove the catalyst, the yields were obtained by gas chromatographic analyses. The organic products were characterized and identified according to the literature.

2.5. X-ray structure determination of 2

Red single crystals of **2** suitable for X-ray diffraction were grown at room temperature from CH_3CN. The crystal, 0.16 × 0.10 × 0.06 mm, was mounted in a capillary tube. All measurements were made on an Enraf Nonius CAD-4/Turbo diffractometer with a graphite monochromated Mo Kα (Kα1; $\lambda = 0.70930$ Å, Kα2; $\lambda = 0.7135$ Å). The final unit-cell parameters were determined to be $a = 7.597(2)$ Å, $b = 14.805(5)$ Å and $c = 24.194(4)$ Å by least-squares refinement of well-centered 25 reflections. The intensity standard was recorded every 60 min during data collection. The data were modified for Lorentz polarization effects and decay. Empirical absorption correction with Ψ-scan was applied to the data. The structure was solved via the conventional heavy-atom method as well as Fourier difference techniques and refined on F by means of full-matrix least-squares procedures using Molen. The

Table 1
Crystallographic data and refinement of the structure for **2**

Empirical formula	$Cu_1Fe_2P_1F_6N_4C_{28}H_{28}$
F_w	740.761
Crystal system	orthorhombic
Space group	$P2_12_12_1$ (#19)
Z	4
Cell parameters	
a (Å)	7.597(2)
b (Å)	14.805(5)
c (Å)	24.194(4)
V (Å^3)	2721(1)
D_{calc} (g cm^{-3})	1.810
μ (cm^{-1} with Mo Kα)	19.6
Transmission factor	81.5–99.7
Scan type	$\omega/2\theta$
Scan width (ω) (°)	1.22 + 0.57 tan(θ)
$2\theta_{max}$ (°)	52.64
No. of reflections measured	3171
No. of reflections observed ($I > 3\sigma(I)$)	883
F(000)	1496
No. of variables	204
Discrepancy indices	
R^a	0.080
R_w^b	0.083
Goodness-of-fit indicator[c]	2.04
Maximum shift in final cycles	less than 0.01

[a] $R = \Sigma||F_o| - |F_c||/\Sigma|F_o|$.
[b] $R_w = [\Sigma w(|F_o| - |F_c|)^2/\Sigma w(F_o^2)]^{1/2}$, where $w = [\sigma F^2 + (0.02F)^2 + 1.00]^{-1}$.
[c] Estimated standard deviation of an observation of unit weight: $[\Sigma w(|F_o| - |F_c|)^2/(N_o - N_v)]^{1/2}$, where N_o = number of observations and N_v = number of variables.

Table 2
Final atomic fractional coordinates and thermal parameters for **2**[a]

Atom	x	y	z	B (Å^2)
Cu(1)	0.8225(7)	0.0428(3)	0.1370(2)	4.1(1)
Fe(1)	0.5499(6)	0.1626(3)	0.2681(2)	2.6(1)
Fe(2)	1.1114(7)	−0.0825(3)	0.0066(2)	2.9(1)
N(1)	0.576(4)	0.106(1)	0.123(1)	3.0(7)
N(2)	0.924(3)	0.031(2)	0.214(1)	3.6(7)
N(3)	0.860(3)	−0.107(2)	0.139(1)	3.9(7)
N(4)	0.907(3)	0.120(2)	0.070(1)	3.4(7)
C(1)	0.288(4)	0.162(2)	0.242(1)	3.3(8)[b]
C(2)	0.300(4)	0.125(2)	0.299(1)	2.8(8)[b]
C(3)	0.414(5)	0.050(2)	0.297(1)	3.4(8)[b]
C(4)	0.489(4)	0.034(2)	0.241(1)	3.1(7)[b]
C(5)	0.405(4)	0.107(2)	0.207(1)	2.6(7)[b]
C(6)	0.821(4)	0.158(2)	0.268(1)	3.5(7)[b]
C(7)	0.746(4)	0.226(2)	0.227(1)	2.7(8)[b]
C(8)	0.646(4)	0.296(2)	0.253(1)	1.9(7)[b]
C(9)	0.651(6)	0.276(3)	0.313(2)	7(1)[b]
C(10)	0.750(4)	0.191(2)	0.321(1)	3.6(9)[b]
C(11)	0.852(4)	−0.093(2)	0.007(1)	2.0(7)[b]
C(12)	0.926(4)	−0.160(2)	0.044(1)	2.6(7)[b]
C(13)	1.033(4)	−0.213(2)	0.009(1)	3.2(8)[b]
C(14)	1.022(5)	−0.184(2)	−0.046(1)	4.1(9)[b]
C(15)	0.914(5)	−0.107(2)	−0.046(1)	4.7(9)[b]
C(16)	1.366(5)	−0.044(2)	−0.014(1)	4.0(8)[b]
C(17)	1.245(5)	0.029(2)	−0.023(1)	4.2(9)[b]
C(18)	1.170(4)	0.043(2)	0.028(1)	2.2(6)[b]
C(19)	1.223(5)	−0.012(2)	0.068(1)	3.5(8)[b]
C(20)	1.357(4)	−0.071(2)	0.041(1)	1.7(7)[b]
C(21)	0.922(4)	−0.165(2)	0.103(1)	2.2(7)[b]
C(22)	1.027(5)	0.112(2)	0.033(1)	3.2(8)[b]
C(23)	0.441(5)	0.130(2)	0.153(1)	3.7(8)[b]
C(24)	0.908(4)	0.070(2)	0.259(1)	2.8(7)[b]
C(25)	1.012(4)	−0.058(2)	0.220(1)	2.4(7)[b]
C(26)	0.894(5)	−0.125(2)	0.199(1)	43(9)[b]
C(27)	0.589(4)	0.150(2)	0.066(1)	3.3(8)[b]
C(28)	0.765(4)	0.193(2)	0.060(1)	2.4(7)[b]
P(1)	0.189(3)	0.376(1)	0.1204(7)	10.6(s)[b]
F(1)	0.281(8)	0.366(4)	0.183(2)	25(2)[b]
F(2)	0.480(8)	0.108(4)	0.854(2)	25(2)[b]
F(3)	0.146(6)	0.472(3)	0.117(1)	17(1)[b]
F(4)	0.386(7)	0.377(3)	0.103(2)	20(2)[b]
F(5)	0.157(9)	0.322(4)	0.068(2)	26(2)[b]
F(6)	0.113(9)	0.283(4)	0.142(3)	28(2)[b]

[a] Estimated standard deviations in the last significant digits, as observed from theleast-squares refinement, are given in parentheses.
[b] Starred atoms were refined isotropically. B values for anisotropically refined atoms are given in the form of the equivalent isotropic displacement parameter defined as: $B = (4/3)[a_2 \times B(1,1) + b_2 \times B(2,2) + c_2 \times B(3,3) + ab(\cos\ \gamma) \times B(1,2) + ac(\cos\ \beta) \times B(1,3) + bc(\cos\ \alpha) \times B(2,3)]$.

Table 3
Selected bond distances (Å) and angles (°) for **2**

Bond distances					
Cu–N(1)	2.12(3)	Fe(1)–C(10)	2.03(4)	N(2)–C(24)	1.25(4)
Cu–N(2)	2.02(3)	Fe(2)–C(11)	1.98(3)	N(2)–C(25)	1.49(4)
Cu–N(3)	2.24(3)	Fe(2)–C(12)	2.04(4)	N(3)–C(21)	1.31(4)
Cu–N(4)	2.09(3)	Fe(2)–C(13)	2.03(2)	N(3)–C(26)	1.48(5)
Fe(1)–C(1)	2.09(4)	Fe(2)–C(14)	2.09(4)	N(4)–C(22)	1.27(4)
Fe(1)–C(2)	2.12(4)	Fe(2)–C(15)	2.00(4)	N(4)–C(28)	1.54(4)
Fe(1)–C(3)	2.08(4)	Fe(2)–C(16)	2.07(4)	C(5)–C(23)	1.38(5)
Fe(1)–C(4)	2.06(4)	Fe(2)–C(17)	2.06(4)	C(6)–C(24)	1.47(5)
Fe(1)–C(5)	2.02(4)	Fe(2)–C(18)	1.98(4)	C(12)–C(21)	1.42(4)
Fe(1)–C(6)	2.06(4)	Fe(2)–C(19)	2.01(4)	C(25)–C(26)	1.43(5)
Fe(1)–C(7)	2.03(4)	Fe(2)–C(20)	2.05(3)	C(18)–C(22)	1.50(5)
Fe(1)–C(8)	2.13(3)	N(1)–C(23)	1.29(5)	C(27)–C(28)	1.48(5)
Fe(1)–C(9)	2.14(5)	N(1)–C(27)	1.53(4)		
Bond angles					
N(1)–Cu–N(2)	121.(1)	N(3)–Cu–N(4)	122.(1)		
N(1)–Cu–N(3)	1 24.(1)	Cu–N(1)–C(27)	106.(3)		
N(1)–Cu–N(4)	85.(1)	Cu–N(4)–C(28)	107.(2)		
N(2)–Cu–N(3)	81.(1)	Fe(2)–C(18)–C(22)	120.(2)		
N(2)–Cu–N(4)	130.(1)				

final cycle of refinement was converted with $R = 0.080$ and $R_w = 0.083$, where w is $[F^2 + (0.02F)^2 + 1.00]^{-1}$. The shift:error ratio in the last cycle of least-squares is less than 0.01 for all parameters. Crystal data, details of the data collection and refinement of the structure are listed in Table 1. Final positional parameters and temperature factors, bond lengths and angles are listed in Tables 2–4.

3. Results and discussion

3.1. Synthesis and characterization

The Cu(I) complexes **2** and **3** incorporating the ligands **1** and dppf, respectively, were formed according to the simple substitution reaction represented by Eq. (1).

$$[Cu(MeCN)_4]PF_6 + L \xrightarrow{CH_2Cl_2} [Cu(L)_x(MeCN)_y]PF_6 \quad (1)$$

2: L = **1**; $x = 1$; $y = 0$

3: L = dppf; $x = 1$; $y = 2$

Here, in connection with the reaction of dppf, it is worth noting that while the addition of the stoichiometric amount of this ligand yielded the expected product (**3**), yet further substitution to give the tetrasubstituted compound of the type $[Cu(dppf)_2]PF_6$ did not take place. The reason may be due to the severe steric congestion caused by two molecules of the bulky ligand around the tetrahedral geometry of the central metal.

Both complexes were characterized by elemental analyses, spectroscopic (IR, NMR), and X-ray crystallography in the case of **2**.

Elemental analyses are consistent with calculated ones, and the ^{1}H NMR spectra of the ligands and complexes are straightforward. As noted in our previous communication [26], the ligand **1** possesses two diastereotopic pairs of aldehydic imine protons ($\delta = 8.21$, 8.04 ppm), which can be confirmed by its X-ray crystal structure [48]. Upon complexation, however, all these protons become equivalent in a tetrahedral geometry around the central metal in **2**, thus exhibiting only one

Table 4
Macrocycle torsion angles (°) for **2**

Atom 1	Atom 2	Atom 3	Atom 4	Angle
N(1)	C(27)	C(28)	N(4)	56(3)
N(2)	C(25)	C(26)	N(3)	61(3)
C(23)	N(1)	C(27)	C(28)	127(3)
C(27)	N(1)	C(23)	C(5)	−174(3)
C(25)	N(2)	C(24)	C(6)	−177(3)
C(24)	N(2)	C(25)	C(26)	122(3)
C(26)	N(3)	C(21)	C(12)	−173(3)
C(21)	N(3)	C(26)	C(25)	111(3)
C(28)	N(4)	C(22)	C(18)	−173(3)
C(1)	C(5)	C(23)	N(1)	157(3)
C(4)	C(5)	C(23)	N(1)	−16(6)
C(24)	C(6)	C(7)	C(8)	170(3)
C(24)	C(6)	C(10)	C(9)	−173(3)
C(7)	C(6)	C(24)	N(2)	−6(6)
C(10)	C(6)	C(24)	N(2)	159(3)
C(15)	C(11)	C(12)	C(21)	169(3)
C(21)	C(12)	C(13)	C(14)	−172(3)
C(11)	C(12)	C(21)	N(3)	−4(6)
C(13)	C(12)	C(21)	N(3)	163(3)
C(16)	C(17)	C(18)	C(22)	−177(3)
C(22)	C(18)	C(19)	C(20)	176(3)
C(18)	C(18)	C(22)	N(4)	158(4)
C(19)	C(18)	C(22)	N(4)	−17(6)

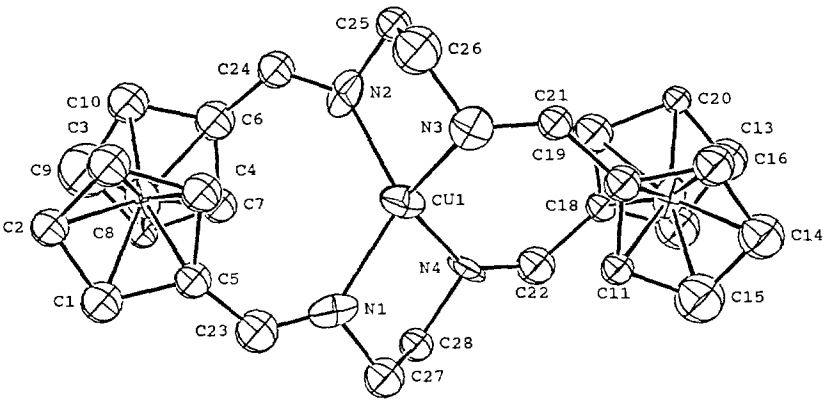

Fig. 1. X-ray crystal structure of **2**.

singlet at a little downfield ($\delta = 8.57$ ppm). The pattern of disubstituted Cp rings is as usual.

The most interesting feature concerning **3** is the appearance of the phosphorus signal in an exceptionally high field ($\delta = -11.87$) as compared with both the free ligand [53] and its analogues incorporating other chelating phosphines such as $R_2PCH_2CH_2PR_2$ (R = Ph, Cy) [54,55], although these observations are not unprecedented as found with other Rh(I) [56] and Cu(I) [57] complexes incorporating the same ligand. At any rate, the increased electron density on the phosphorus atoms exerted by the filled *d*-orbitals of Cu(I) may be responsible for this shift.

Both **1** and **2** show the characteristic imine stretching bands ($\nu_{C=N}$) in the region of 1609–1639 cm^{-1} which move to lower frequency upon complexation. The compound **3** shows a pair of weak bands at 2306 and 2271 cm^{-1} assignable to the stretching bands of the coordinated acetonitrile.

3.2. X-ray crystal structure of 2

In order to obtain more systematic structural information, the X-ray crystal structure of **2** has been determined whose ORTEP view is shown in Fig. 1. A summary of the crystallographic data and refinement results, final atomic coordinates for nonhydrogen atoms, and selected bond distances and angles are listed in Tables 1–4.

The copper(I) ion possesses a distorted tetrahedral geometry with the Cu–N1 and Cu–N3 bonds being on average some 0.13 Å longer than the Cu–N2 and Cu–N4 bonds. Bond distances of copper atom to neighboring nitrogen atoms (average of 2.12 Å) is slightly longer than those (average of 2.047 Å) found in the related copper(II) complex [42].

The smallest bond angle around the copper atom in the five- membered rings is 81.(1)° for N2–Cu–N3 due to the geometrical constraints in the coordinated tetraazamacrocyclic ligand which contains ethylenediamine moieties. The macrocycle torsional angles are shown in Table 4. The CuN1C27C28N4 and CuN2C25C26N3 rings adopt the usual chair conformation (the torsional angle N1–C27–C28–N4 is 56(3)° and N2–C25–C26–N3 is 61(3)°).

Fe–C(cyclopentadienyl ring) distances range from 1.98(3) to 2.14(5) Å (average of 2.05 Å) and intracyclopentadienyl C–C bond lengths lie in the range 1.33(4)–1.53(5) Å (average of 1.44 Å). These bond length variations lead to the small deviations from the ring planarity of cyclopentadienyl rings. Cyclopentadienyl rings are rotated by 28(2)° and 26(2)° from exactly eclipsed conformation at Fe(1) and Fe(2), respectively.

3.3. Catalysis

In spite of numerous examples for copper macrocycles [38–41] and their reaction chemistry with small molecules such as carbon monoxide [37,58], olefins [58] and carbon dioxide [59], their use as homogeneous catalyst in organic synthesis via the activation of these small molecules are rare. Such examples include catalytic oxidation with dinuclear Cu(II) macrocyclic dioxygen complexes [60–63], epoxydation of styrene by Cu(II) macrocycles [64].

Here, we report for the first time, the use of a cationic copper(I) complex incorporating the ferrocene-containing tetraazamacrocycle for the incorporation of CO_2 in the catalytic formation of carbamates and cyclic carbonates. As mentioned previously, catalytic formation of carbamates and cyclic carbonates from the reaction of acetylenic alcohol derivatives with CO_2 is well established [4,5].

In the present work, the same reactions represented by Eq. (2) were carried out employing the cationic

copper complex **2** as catalyst and other compounds for comparative purposes.

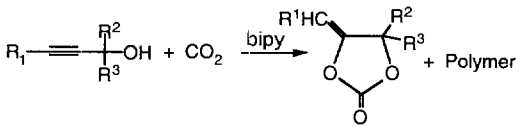

4 5

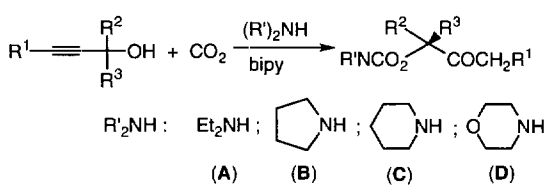

(2)

(A) (B) (C) (D)

Tables 5 and 6 present the yields of various carbamates and cyclic carbonates, respectively, under a standard set of conditions. Both tables show that our new copper(I) complex **2** is an excellent catalyst giving almost quantitative product yields in most cases. These results are among the highest yields reported in Refs. [4,5,19].

For unknown reasons, the presence of substituents (R^2 and R^3) other than hydrogen at the α-carbon of the propargyl alcohol seems to be essential to maintain high product yields as can be seen from entry 1 of Table 5 and entries 13–16 of Table 6. A dramatic example for these observations is the exclusive formation of a polycarbonate instead of the desired cyclic carbonate as shown in entry 1 of Table 5. The polymer formation from this reaction was confirmed by comparing the infrared pattern of the product with that of related polycarbonates obtained under different catalytic conditions [51,52]. Comparison of molecular weights and other spectroscopic data such as NMR, however, could not be made due to the insolubility of our product in any organic solvent.

The yields drop also when the terminal acetylenic hydrogen is replaced by other bulkier substituents, which may be explained in terms of steric hindrance. These observations are demonstrated in entry 5 of Table 5 and entries 17–20 of Table 6.

Table 5
Yields of cyclic carbonates catalyzed by **2**[a]

Entry	Substrate			Yield (%)[b]	
	R^1	R^2	R^3	**4**	**5**
1	H	H	H	–	> 95
2	H	Me	Me	94	–
3	H	Me	Et	96	–
4	H	Me	Ph	90	–
5	Ph	Me	Me	0	–

[a]Reaction conditions: [substrate] = 5 mmol (neat); [catalyst] = 0.05 mmol; [bipy] = 0.5 mmol; $P(CO_2)$ = 38 atm; reaction temperature = 100°C; reaction time = 24 h.
[b]GC yield based on the substrate.

Table 6
Yields of carbamates catalyzed by **2**[a]

Entry	Substrate			Amine	Yield (%)[b]
	R^1	R^2	R^3		
1	H	Me	Me	**A**	96
2				**B**	100
3				**C**	100
4				**D**	96
5	H	Me	Et	**A**	94
6				**B**	90
7				**C**	94
8				**D**	80
9	H	Me	Ph	**A**	94
10				**B**	84
11				**C**	94
12				**D**	80
13	H	H	H	**A**	57
14				**B**	44
15				**C**	40
16				**D**	45
17	Ph	Me	Me	**A**	44
18				**B**	40
19				**C**	35
20				**D**	35

[a]Reaction conditions: [substrate] = 5 mmol (neat); [catalyst] = 0.05 mmol; [bipy] = 0.5 mmol; [amine] = 10 mmol; $P(CO_2)$ 38 atm; reaction temperature = 100°C; reaction time = 24 h.
[b]GC yield based on the substrate.

Some comparative studies have been performed to investigate the role of ligand, metal and counter anion. The results are summarized in Table 7. The complex **2** exhibits the most powerful catalytic activity among those employed, and the comparison with **3** and $[Cu(MeCN)_4]PF_6$ reveals that the strong binding of the tetradentate ligand **1** is crucial. It may be deduced that, although the electronically saturated Cu(I) complex **2** would rather exhibit less reactivity as compared with CuCl due to its steric congestion, the redox active centers derived from multiple ferrocene units may have a role by communicating electronically with the central copper metal to make it more sensitive toward oxidation

Table 7
Some reaction parameters for the yields of cyclic carbonates[a]

Entry	Catalyst	Base	Yield (%)[b]
1	$[Cu(\mathbf{1})]PF_6$(**2**)	bipy	94
2	$[Cu(\mathbf{1})]ClO_4$	bipy	98
3		NEt_3	65
4	**3**	bipy	63
5	$[Cu(MeCN)_4][PF_6]$	bipy	47
6	$Fe_3(CO)_{12}$	bipy	78
7	$Ru_3(CO)_{12}$	bipy	63

[a]Reaction conditions: [substrate] = 5 mmol; [catalyst] = 0.05 mmol; [base] = 0.5 mmol; $P(CO_2)$, 38 kg cm^{-2}; reaction temperature = 100°C; reaction time = 24 h.
[b]GC yield based on the substrate.

to Cu(II). The exact role of the ferrocene moiety in the tetraazamacrocycle in comparison with a simple organic counter part has yet to be investigated further in the future.

The effect of counter anion is insignificant, and for unknown reasons, 2,2′-bipyridine is preferred over NEt_3 which is the common base used by others to activate deprotonation of the substrate alcohol (cf. Scheme 1).

The mechanism for the formation of both products may proceed in a similar manner as described in Scheme 1. The first step of the catalytic cycle is the formation of nucleophilic adduct which then enters into the catalytic cycle by nucleophilic attack on the coordination product formed from the reaction of catalyst with propargyl alcohol. A metalloenolate thus formed completes the cycle to produce carbamates and cyclic carbonates, respectively, through transesterification followed by tautomerization and by intramolecular cyclization. Yet no attempt has been made to isolate any intermediates involved in the cycle.

Acknowledgements

TJK gratefully acknowledges the Korea Science and Engineering Foundation and the Ministry of Education through the Basic Research Program for the financial support.

References

[1] A. Behr, in: W. Keim (Ed.), Catalysis in C_1 Chemistry, Reidel, Dordrecht, 1983.
[2] D.J. Darensbourg, R.A. Kudaroski, Adv. Organomet. Chem. 22 (1983) 129.
[3] R.P.A. Sneeden, in: G. Wilkinson, F.G.A. Stone, E.W. Abel (Eds.), Comprehensive Organometallic Chemistry, Pergamon, New York, 1982.
[4] C. Bruneau, P.H. Dixneuf, in: C.-I. Branden, G. Schneider (Eds.), Carbon Dioxide Fixation and Reduction in Biological and Model Systems, Oxford Science Publ., Oxford, 1994.
[5] C. Bruneau, P.H. Dixneuf, J. Mol. Catal. 74 (1992) 97.
[6] A. Behr, in: M.G. Weller (Ed.), Carbon Dioxide Activation by Metal Complexes, VCH Press, Weinheim, 1988.
[7] B.M. Trost, J.R. Granja, Tetrahedron Lett. 32 (1991) 2193.
[8] C. Darcel, S. Bartsch, C. Bruneau, P.H. Dixneuf, Synlett. 457 (1994) 137.
[9] P. Dimroth, H. Pasedach, E. Schefezik, Ger. Pat. 1 (151) (1964) 507.
[10] P. Dimroth, H. Pasedach, Ger. Pat. 1 (098) (1961) 953.
[11] P. Dimroth, H. Pasedach, Ger. Pat. 1 (164) (1964) 411.
[12] H. Laas, A. Nissen, A. Nurrenbach, Synthesis, 1981, p. 958.
[13] Y. Sasaki, Tetrahedron Lett. 27 (1986) 1573.
[14] Y. Inoue, Y. Itoh, I.F. Yen, S. Imaizumi, J. Mol. Catal. 60 (1990) L1.
[15] Y. Inoue, J. Ishikawa, M. Taniguchi, H. Hashimoto, Bull. Chem. Soc. Jpn. 60 (1987) 1204.
[16] C. Bruneau, P.H. Dixneuf, S. Lecolier, J. Mol. Catal. 44 (1988) 175.
[17] Y. Sasaki, P.H. Dixneuf, J. Org. Chem. 52 (1987) 4389.
[18] C. Bruneau, P.H. Dixneuf, Tetrahedron Lett. 28 (1987) 2005.
[19] T.J. Kim, K.H. Kwon, S.C. Kwon, J.O. Baeg, S.C. Shim, D.H. Lee, J. Organomet. Chem. 389 (1990) 205.
[20] T. Hayashi, in: A. Togni, T. Hayashi (Eds.), Ferrocene, VCH Press, Weinheim, 1995.
[21] R. Noyori, Asymmetric Catalysis in Organic Synthesis, Wiley, New York, 1994.
[22] M. Sawamura, M. Sudoh, Y. Ito, J. Am. Chem. Soc. 118 (1996) 3309.
[23] A. Togni, C. Breutel, A. Schnyder, A. Spindler, H. Landert, A. Tiiani, J. Am. Chem. Soc. 116 (1994) 4062.
[24] W.R. Cullen, F.W.B. Einstein, T. Jones, T.J. Kim, Organometallics 4 (1985) 346.
[25] T.G. Appleton, W.R. Cullen, S.V. Evans, T.J. Kim, J. Trotter, J. Organomet. Chem. 279 (1985) 5.
[26] E.J. Kim, S.C. Kwon, S.C. Shim, J.H. Jeong, T.J. Kim, Bull. Korean Chem. Soc., in press.
[27] C. Kollmar, M. Couty, O. Kahn, J. Am. Chem. Soc. 113 (1991) 7994.
[28] K.M. Chi, J.C. Calbrese, W.M. Reiff, J.S. Miller, Organometallics 10 (1991) 668.
[29] R.W. Wagner, P.A. Brown, T.E. Johnson, J.S. Lindsey, J. Chem. Soc., Chem. Commun., 1991, p. 1463.
[30] E.C. Constable, Angew. Chem., Int. Ed. Engl. 30 (1991) 407.
[31] S.R. Marder, in: D.W. Bruce, D. O'Hare (Eds.), Inorganic Materials, Wiley, Chichester, 1992, p. 115 and references therein.
[32] K.L. Kott, D.A. Higgins, R.J. McMahon, R.C. Corn, J. Am. Chem. Soc. 115 (1993) 5342.
[33] Z. Yuan, N.J. Taylor, Y. Sun, T.B. Marder, I.D. Williams, L.-T. Cheng, J. Organomet. Chem. 449 (1993) 27.
[34] Z. Yuan, G. Stringer, I.R. Jobe, D. Kreller, K. Scott, L. Koch, N.J. Taylor, T.B. Marder, J. Organomet. Chem. 452 (1993) 115.
[35] A. Benito, J. Cano, R. Martinez, J. Paya, J. Soto, M. Julve, F. Lloret, M.D. Marcos, E. Sinn, J. Chem. Soc., Dalton Trans., 1993, p. 1999.
[36] C.D. Hall, in: A. Togni, T. Hayashi (Eds.), Ferrocene, VCH Press, Weinheim, 1995.
[37] F.C.M. van Veggel, W. Verboom, D. Reinhoudt, Chem. Rev. 94 (1994) 279.
[38] P.D. Beer, J.E. Nation, M.E. Harman, M.B. Hursthouse, J. Organomet. Chem. 441 (1992) 465.
[39] P. Beer, O. Kocian, R.J. Mortimer, P. Spencer, J. Chem. Soc., Chem. Commun., 1992, p. 602.
[40] C.D. Hall, N.W. Sharpe, I.P. Danks, Y.P. Sang, J. Chem. Soc., Chem. Commun., 1989, p. 419.
[41] P.D. Beer, M.G.B. Drew, D. Hesek, S.M. Lacy, J. Organomet. Chem. 511 (1996) 207.
[42] A. Benito, J. Cano, R. Martinez-Mañez, J. Soto, J. Paya, F. Lloret, M. Julve, J. Faus, M.D. Marcos, Inorg. Chem. 32 (1993) 1197, and references therein.
[43] P.D. Beer, J.E. Nation, S.L.W. McWhinnie, M.E. Harman, M.B. Hursthouse, M.I. Ogden, A.H. White, J. Chem. Soc., Dalton Trans., 1991, p. 2485.
[44] J.M. Johnson, J.E. Bulkowski, A.L. Rheingold, B.C. Gates, Inorg. Chem. 26 (1987) 2644.
[45] J. Powell, M. Gregg, A. Kuksis, P. Meindl, J. Am. Chem. Soc. 105 (1983) 1064.
[46] J.J. Bishop, A. Davision, M.L. Katcher, D.W. Lichtenberg, R.E. Merril, J.C. Smart, J. Organomet. Chem. 27 (1971) 241.
[47] G.G.A. Balavoine, G. Doisneau, T. Fillebeen-Khan, J. Organomet. Chem. 421 (1991) 381.
[48] M.J.L. Tendero, A. Benito, R.M. Manez, J. Soto, J. Paya, A.J. Edwards, P.R. Raithby, J. Chem. Soc., Dalton Trans., 1996, p. 343.

[49] G.J. Kubas, B. Monzyk, A.L. Crumbliss, Inorg. Synth. 19 (1971) 90.
[50] R. Mahe, Y. Sasaki, C. Bruneau, P. Dixneuf, Org. Chem. 54 (1989) 1518.
[51] M. Yang, M. Zheng, A. Furlani, M.V. Russo, J. Polym. Sci., Part A 32 (1994) 2709.
[52] L. Yamaguchi, K. Osakada, T. Yamamoto, J. Polym. Sci., Part A 34 (1994) 1609.
[53] A.L. Bandini, G. Banditelli, M.A. Cinellu, G. Sanna, G. Minghetti, F. Demartin, M. Manassero, Inorg. Chem. 28 (1989) 404.
[54] D.P. Fairlie, B. Bosnich, Organometallics 7 (1988) 936.
[55] M.M. Taquikhan, E.R. Rao, M.R.H. Siddiqui, B.T. Khan, S. Begun, S.M. Ali, J. Reddy, J. Mol. Catal. 45 (1988) 35.
[56] T.J. Kim, K.C. Lee, Bull. Korean Chem. Soc. 10 (1989) 279.
[57] S.P. Neo, Z.-Y. Zhou, T.C.W. Mark, T.S.A. Hor, J. Chem. Soc., Dalton Trans., 1994, p. 3431.
[58] P. Chaudhuri, K. Oder, J. Organomet. Chem. 367 (1989) 249.
[59] C. Bazzicalupi, A. Bencini, A. Bencini, A. Bianchi, F. Corana, V. Fusi, C. Giorgi, P. Paola, P. Paoletti, V. Barbara, Z. Claudia, Inorg. Chem. 35 (1996) 5540.
[60] A.E. Martell, R.J. Motekaitis, J. Ramunas, R. Menif, D.A. Rockcliffe, A. Liobet, J. Mol. Catal., A: Chem. 117 (1997) 205.
[61] D.A. Rockcliffe, A.E. Martell, Inorg. Chem. 32 (1993) 3143.
[62] D.A. Rockcliffe, A.E. Martell, J. Chem. Soc., Chem. Commun., 1992, p. 1758.
[63] F.V. Acholla, K.B. Mertes, Bull. Chem. Soc. Ethiopia 3 (1989) 17.
[64] Y.C. Park, S.S. Kim, Bull. Korean Chem. Soc. 13 (1992) 458.